International Journal of Thermophysics, Vol. 1, No. 3, 1980

Anharmonic Effects in the Specific Heat of Aluminum

R. C. Shukla[1] **and C. A. Plint**[1]

Received June 30, 1980

The specific heat at constant pressure, C_p, of aluminum has been measured by Leadbetter between 300 and 772 K and by Brooks and Bingham between 330 and 893 K. Both sets of data are converted to the specific heat at constant 0 K volume, C_{v_0}, by the Slater-Overton method, based on the equation of state and not the Debye type of theory. Corrections to the work of Overton are given. Our analysis shows that the C_{v_0} obtained from Leadbetter's data remains below $3R$ up to 750 K, whereas it becomes $>3R$ for the Brooks and Bingham data in the temperature range 650–850 K. Calculations of C_{v_0} (harmonic + anharmonic) from three pseudopotentials are reported for (a) Harrison modified point ion potential with Hubbard exchange and correlation factor in the dielectric function, $\epsilon(q)$; (b) Ashcroft pseudopotential with the same $\epsilon(q)$ as in (a); and (c) Dagens–Rasolt–Taylor (DRT) M2 pseudopotential with Geldart–Taylor $\epsilon(q)$. The shape of the C_{v_0} curve is found to be similar for all three potentials. For DRT potential, C_{v_0} reaches $3R$ at 700 K, whereas the other two barely approach $3R$ about 900 K. The anharmonic contribution to C_{v_0} is a factor of two larger for the Dagens et al. compared to the other two potentials. There is a marked difference between the C_{v_0} curve from the analysis of the Brooks and Bingham data and the theoretical curves. It appears that the experimental points are too high from about 500 K up. The C_{v_0} curve from Leadbetter's data is very similar to the three theoretical curves, but the results appear to be too low. A remeasurement of the specific heat from 500 K to the melting point is needed.

KEY WORDS: Helmoltz free energy; anharmonic aluminum fcc Crystal; constant pressure and constant volume specific heat; interionic potentials for aluminum; equation of state; perturbation theory.

1. INTRODUCTION

The specific heat at constant pressure, C_p, of aluminum has been measured by Leadbetter [1] for temperatures between 300 and 772 K and by Brooks and

---

[1] Physics Department, Brock University, St. Catharines, Ontario L2S 3A1, Canada.

Bingham [2] between 330 and 893 K. Since anharmonic effects are expected to be important from the Debye temperature, Θ_D, to the melting point (420 and 933 K, respectively, for aluminum), both Leadbetter [3] and Brooks and Bingham [2] have examined the anharmonic contributions to the specific heat at constant volume, C_v^A, after conversion of C_p to C_v by the standard thermodynamic relation and subtraction of the harmonic C_v based on the Debye model. In Leadbetter's analysis [3], it is found that C_v^A has a linear temperature dependence of the form $3NAk_BT$, where N is the Avogadro number, k_B is the Boltzmann constant, and A is the anharmonic coefficient. This form of C_v^A [4–8] arises from the high temperature limit ($T > \Theta_D$) of the two lowest-order perturbation theory terms in the anharmonic Helmholtz free energy, F_3 and F_4, which are themselves dependent on the cubic and quartic terms in the Taylor expansion of the crystal potential energy. Leadbetter's analysis led to a negative sign for the coefficient A, so that the value of C_v is less than the high temperature limit of the harmonic contributions to C_v, viz. $3R$. In contrast, for C_v^A, the analysis of Brooks and Bingham [2] gave a result opposite to that of Leadbetter. In the high temperature limit, C_v was greater than $3R$.

In order to compare the experimental value of C_v at temperature T and volume $V(T)$ with the results of theory, the experimental value $C_v(T, V(T))$ should be reduced to the value $C_v(T, V(0))$ corresponding to a volume $V(0) \equiv V_0$ that is fixed at the 0 K value. Leadbetter [3] alone made this reduction in his analysis. In light of the differences between the results of the examination of the two sets of data, it is worthwhile to make a fresh analysis of the data sets by a common method.

In this paper, we present an analysis of the two sets of C_p data for aluminum and convert $C_v(T, V(T))$ to $C_{v_0}(T)$ using a method introduced by Slater [9] and further developed by Overton [10]. Some corrections to the equations as published in ref. [10] are given. The experimental $C_{v_0}(T)$ is then compared with the results of calculations of C_{v_0} (harmonic and anharmonic) using a wide variety of two body potentials, $V(r)$, such as the phenomenological Morse and Rydberg potentials and the more fundamental potentials based on the pseudopotential theory of metals. From the latter group, we have selected three potentials for the calculation of F_3, F_4, and C_v^A for aluminum:

a. Harrison modified point-ion potential [11] with Hubbard-Sham exchange and correlation correction factor in the dielectric function $\epsilon(\mathbf{q})$.
b. Ashcroft pseudopotential with Hubbard form for exchange and correlation correction factor in $\epsilon(\mathbf{q})$.
c. The model pseudopotential of Dagens et al. [12] with Geldart–Taylor exchange and correlation correction factor in $\epsilon(\mathbf{q})$.

We have made the above choices for aluminum because potential (a) was used by Koehler et al. [13] in their anharmonic calculations of phonon widths and shifts; Monte Carlo results for C_v at 500, 600, and 700 K are available from the calculations of Mountain and Knauss [14] for potential (b); and potential (c) is a first principles type without adjustable parameters in either the pseudopotential or in the screening function. Finally, it should be noted that the phonon dispersion curves calculated from the first and second derivatives of these three potentials show good agreement with the experimental results [15] along the principal symmetry directions, thereby indicating that there is little difference in the first two derivatives. Since the calculation of F_3 and F_4 requires knowledge of frequencies, eigenvectors, and the first four derivatives, any differences in the results for C_v^A should be due to differences in the third and fourth derivatives of these potentials.

The plan of this paper is as follows. In Section 2 we present the reduction of C_v to C_{v_0} by Slater's method and the corrections required in the Overton formulas. The summary of the above mentioned potentials is given in Section 3. The anharmonic calculations of F_3, F_4, and C_v^A, employing the method of Shukla and Taylor [16] for the long range potentials, is presented in Section 4. The discussion of the theoretical and experimental results of C_v and C_v^A is presented in Section 5, and finally, the conclusions are stated in Section 6.

2. REDUCTION OF THE SPECIFIC HEAT

The experimental specific heat at constant pressure is converted to the specific heat at constant volume by the standard formula

$$C_v = C_p - TV\beta^2 B \tag{1}$$

where B is the isothermal bulk modulus, β is the coefficient of volume expansion, and T is the thermodynamic temperature. The specific heat at the constant volume V_0 is related to the specific heat at the volume V occupied at temperature T by

$$C_v(T, V_0) = C_v(T, V) - \int_{V_0}^{V} (\partial C_v/\partial V)_T dV \tag{2}$$

The integrand in this equation can be replaced by the equivalent form $T(\partial^2 p/\partial T^2)_v$ and the integral evaluated if $p(V, T)$ is known. Slater [9] described a method for the evaluation, which has been extended by Overton [10]. It should be noted that the method does not depend on any assumptions regarding quasiharmonic frequency distribution or other features of the modified Debye model [3]. The accuracy of the final specific heat determination, $C_{v_0}(T)$, is limited only by the small approximations involved in the Slater–Overton treatment and the accuracy of the experimental data that constitute the equation of state.

When the equation of state is written in Bridgman's form,

$$V(T,p) = V(T,0)[1 - a_1(T)p + a_2(T)p^2 + \cdots] \tag{3}$$

the integral in Eq. (2) is replaced by

$$\begin{aligned}(a_0V_0T)^{-1}E(T) = &-(\beta^2/k)\left[1 + 5x - \frac{2a_2}{k^2} - \frac{a_0(1+6x)}{2(1+a_0)} - \frac{a_0a_2(a_0+6)}{3k^2(1+a_0)^2}\right]\\ &+(\beta'/k)\left[1 + x - \frac{a_0(1+2x)}{2(1+a_0)} + \frac{a_0{}^2a_2}{3k^2(1+a_0)^2}\right]\\ &-(\beta k'/k^2)\left[2 + 6x - \frac{a_0(1+6x)}{(1+a_0)} + \frac{2a_0{}^2a_2}{k^2(1+a_0)^2}\right]\\ &+\frac{a_0\beta a_2'[2 + 2/3a_0]}{k^3(1+a_0)^2} + \frac{a_0(k')^2(1+4x)}{(1+a_0)k^3}\\ &-\frac{2a_0{}^2a_2'k'}{(1+a_0)^2k^4} - \frac{a_0k''(1+2x)}{2k^2(1+a_0)} + \frac{a_0{}^2a_2''}{3k^3(1+a_0)^2}\end{aligned} \tag{4}$$

where $a_0 = (V - V_0)/V_0$, $\beta = (1/V)\ (\partial V/\partial T)_p$, $k = -(1/V)\ (\partial V/\partial p)_T$, $x = a_0a_2/k^2\ (1 + a_0)$, the primes represent derivatives with respect to temperature at constant pressure, and $E(T)$ is the integral in Eq. (2). In this form, the formula for $E(T)$ is suitable for use when accurate data for V, β, β', and the coefficients a_1 and a_2 of the equation of state are available. An alternative form of the formula can be written in terms of the coefficient of volume expansion, the isothermal bulk modulus, and their derivatives. This form is suitable for use when accurate measurements of elastic constants, from which the bulk modulus is derivable, are available.

The alternative form is obtained from Eq. (4) by the substitutions

$$a_2 = (W + 1)/2B^2$$

$$a_2' = W'/2B^2 - B'(W + 1)/B^3$$

$$a_2'' = W''/2B^2 - 2W'B'/B^3 + 3(B')^2(W + 1)/B^4 - B''(W + 1)/B^3$$

in which $B = 1/k$, $W = (\partial B/\partial p)_T$, and the primes denote differentiation with respect to temperature at constant pressure:

$$\begin{aligned}(a_0V_0T)^{-1}E(T) = {} & \beta^2B\left[W + \frac{a_0(1 - 10x/3)}{2(1 + a_0)} - \frac{3x}{1 + a_0}\right] \\ & + \beta'B\left[1 + x - \frac{a_0(1 + 4x/3)}{2(1 + a_0)}\right] \\ & + \beta B'\left[2 + 6x - \frac{a_0(1 + 16x/3)}{1 + a_0} - \frac{4x}{1 + a_0}\right] \\ & + B''\frac{a_0(1 + 2x/3)}{2(1 + a_0)} + \frac{BW''a_0^2}{6(1 + a_0)^2} \\ & + B\beta W'\frac{a_0(1 + a_0/3)}{(1 + a_0)^2} + \frac{W'B'a_0^2}{3(1 + a_0)^2} \end{aligned} \tag{5}$$

where x is now expressed as $a_0(1 + W)/2(1 + a_0)$. We have presented Eqs. (4) and (5) in full because of errors in the equivalent Eqs. (12) and (18) in Overton's paper [10].

For the range of temperature of interest for this work, values of the isothermal bulk modulus and its derivatives can be obtained from the adiabatic elastic constants determined by ultrasonic measurements. Conversion of the adiabatic bulk modulus and its derivatives, denoted by the subscript s, to the isothermal values is made by use of the standard formula,

$$1/B = 1/B_s + TV\beta^2/C_p \tag{6}$$

and the result of Overton [17],

$$W = W_s + Z(1 - 2B'/B\beta - 2W_s) + Z^2(W_s - 1 - \beta'/\beta^2) \tag{7}$$

$$Z = TV\beta^2B/C_p \tag{8}$$

in which some errors in the published formulas have been corrected.

The specific heat at the 0 K volume is then given by $C_v(T, V) - E(T)$. For the lattice specific heat, the electronic contribution corresponding to the fixed volume V_0 at temperatures T must be subtracted. At sufficiently high temperatures, a further correction for the contribution of vacancy formation is required.

In determining the value of C_{v_0} by application of Eqs. (1)–(5), the following data sources were used:

$\beta(T < 300$ K), Fraser and Hollis-Hallet [18] and Gibbons [19], ±1%
$\beta(T > 300$ K), Simmons and Balluffi [20], ±1%
$B_s(T > 300$ K), Gerlich and Fisher [21], ±1%

$W_s(T > 300$ K), Thomas [22] and Schmunk and Smith [23], ±4%

$C_p(T > 300$ K), Leadbetter [1], 0.2%, Brooks and Bingham [2], 0.6%

These data are similar to those used by Leadbetter [3] with two exceptions. For the modulus B_s, the measurements of Gerlich and Fisher [21] are used rather than an extrapolation of the low temperature data [3]. For W_s, the data of Thomas [22] differs appreciably from that of Schmunk and Smith [23] as used by Leadbetter [3]. We have used the mean of the two values in the analysis presented in Section 5. Our error estimates for β, B_s, and W_s are indicated alongside the sources, whereas for C_p, the estimates of the original authors are shown.

In the reduction of C_p to C_{v_0} for the two sets of data [1, 2], the values of V, β, β', B_s, and W_s remain unchanged. First, we calculate the values of V, β, and β' from the macroscopic expansivity data of Simmons and Balluffi [20]. Next, a smooth set of values of V, β, and β' are obtained from a third degree polynomial fit of V versus T. These values of V, β, and β', along with values of B_s, in the temperature range $300 \leq T \leq 850$ K, are presented in Table I.

3. POTENTIAL FUNCTIONS FOR Al

Several two body potentials, $\Phi(r)$, have been constructed for Al employing different pseudopotentials (local and nonlocal) and electron gas screening functions, $\epsilon(\mathbf{q})$. The effect of different $\epsilon(\mathbf{q})$'s on $\Phi(r)$, for Al, has been examined by Duesbery and Taylor [24] and Rao [25]. Essentially, the

Table I. Values of the Volume V (m$^3 \cdot$ kg^{-1}), Coefficient of Expansion β (K^{-1}), β' (K^{-2}), and the Adiabatic Bulk Modulus B_s (Pa) Used in the Reduction of the Experimental Data[a]

T (K)	V $\times 10^4$	β $\times 10^5$	β' $\times 10^8$	B_s $\times 10^{-10}$
300	3.7069	6.73	5.65	7.571
350	3.7196	7.02	5.89	7.491
400	3.7330	7.32	6.12	7.399
450	3.7470	7.63	6.35	7.299
500	3.7616	7.95	6.57	7.201
550	3.7769	8.29	6.78	7.093
600	3.7929	8.63	6.99	6.991
650	3.8096	8.99	7.18	6.880
700	3.8271	9.35	7.37	6.769
750	3.8454	9.72	7.55	6.659
800	3.8645	10.10	7.73	6.545
850	3.8845	10.50	7.89	6.418

[a] The quantity $W_s = (\partial B_s/\partial p)_T = 4.50$ is taken from ref. [22] and is independent of temperature. $V_0 = 3.6598 \times 10^{-4}$ (m$^3 \cdot$ kg^{-1}).

potentials thus obtained are very similar in their behavior, except in the neighborhood of first and second neighbor positions. For example, in ref. [25], a deep minimum in $\Phi(r)$ is obtained in the region of the nearest neighbor distance (r_1) with the Hubbard $\epsilon(\mathbf{q})$ (which includes exchange effects). On the other hand, no minimum in $\Phi(r)$ is obtained with the Hartree $\epsilon(\mathbf{q})$ (which excludes exchange effects) in the region of r_1. When both the correlation and exchange effects are included in $\epsilon(\mathbf{q})$, such as in the $\epsilon(\mathbf{q})$'s of Singwi et al. [26] (SSTL), and Geldart and Taylor [27] (GT), the calculation of Duesbery and Taylor [24] shows a deep minimum in $\Phi(r)$ just beyond r_1 with the SSTL $\epsilon(\mathbf{q})$ as compared to no minimum in $\Phi(r)$ for the GT $\epsilon(\mathbf{q})$. The essential difference in the GT and SSTL $\epsilon(\mathbf{q})$ is that the former satisfies the compressibility sum rule, whereas the latter does not. For the more recent version of SSTL, that of Vashishta and Singwi [28], $\epsilon(\mathbf{q})$ gives no minimum in $\Phi(r)$ near r_1 [25]. The essential points of the above summary are reflected in the choice of the three potentials summarized below, all of which can be written in the following form:

$$\Phi(r) = \frac{z^2e^2}{r} - \frac{2z^2e^2}{\pi}\int_0^\infty G(q)\,\frac{\sin qr}{qr}\,\mathrm{d}q \tag{9}$$

where e is the electronic charge and z is the valence. The first term in Eq. (9) represents the direct ion–ion coulomb interaction, and the second term represents the ion–electron interaction as screened by the other electrons. The function $G(q)$ includes the exchange and correlation effects. In fact, there is a third contribution in $\Phi(r)$ due to the overlap of the ion core wave functions, repulsive in nature, but it has been found to be negligible in Al [29] and we neglect it here. The expressions of $G(q)$ for the different cases mentioned above in the introduction are as follows.

First, we consider the Harrison modified point-ion potential with Hubbard–Sham $\epsilon(\mathbf{q})$:

$$G(q) = \left[\frac{\Omega q^2}{4\pi z e^2}\,V_b(q)\right]^2\left[\frac{\epsilon_q - 1}{1 + (\epsilon_q - 1)(1 - g_q)}\right] \tag{10}$$

$$V_b(q) = \left(\frac{1}{\Omega}\right)\left[-\frac{4\pi z e^2}{q^2} + \frac{\beta}{(1 + q^2\rho^2)^2}\right] \tag{11}$$

$$g_q = q^2/[2(q^2 + \xi k_F{}^2)] \tag{12}$$

where in Eqs. (10)–(12), Ω is the atomic volume, ϵ_q is the Hartree dielectric function, and $(1 - g_q)$ is the Hubbard–Sham exchange and correlation factor. The parameter ξ is determined from the compressibility of the electron gas, and k_F is the Fermi radius. The pseudopotential parameters β and ρ in the bare-ion pseudopotential $V_b(q)$ and the parameter ξ in g_q have been determined by Koehler et al. [13] and Wallace [29], and their values are given by

$$\beta = 47.5\, a_0^3\, (Ry), \quad \rho = 0.24\, a_0, \quad \xi = 1.90$$

where a_0 is the Bohr radius.

Second, we consider the Ashcroft pseudopotential with Hubbard ϵ ($\mathbf{q}$) [14],

$$G(q) = \cos^2(qr_c)\left(1 - \frac{1}{\epsilon(q)}\right) \tag{13}$$

$$\epsilon(q) = 1 + \frac{Q_0(q)}{[1 - f(q)Q_0(q)]} \tag{14}$$

$$Q_0(q) = (k_{TF}{}^2/q^2)F(\eta) \tag{15}$$

$$F(\eta) = \frac{1}{2} + \left(\frac{4 - \eta^2}{8\eta}\right)\ln\left|\frac{2 + \eta}{2 - \eta}\right| \tag{16}$$

where, in Eqs. (15) and (16), $\eta = q/k_F$, $k_{TF}^2 = (m^*/m)\,(4k_F/\pi a_0)$, and m^* is the effective electron mass. The function $f(q)$ appearing in Eq. (14) is identical to g_q defined by Eq. (12), but now $\xi = 1.699$. The core radius r_c in Eq. (13) is given a value $1.12\, a_0$, and $(m^*/m) = 1$.

Third, we consider the model pseudopotential of Dagens et al. with Geldart–Taylor $\epsilon(\mathbf{q})$. Dagens et al. [12] have carried out a nonlinear self-consistent calculation of the charge density induced by an isolated Al^{3+} ion placed in an electron gas of the appropriate metallic density, and they have calculated the Al interionic potential. The GT screening function was used in their calculations of the phonon dispersion curves of Al. The details of the Al model potential and its parameters can be obtained from refs. [12, 30]. In this work, we have used their M2 model potential.

4. CALCULATION OF F_3 AND F_4

The formal expressions for F_3 and F_4, suitable for computation involving long range interactions, have been presented before in ref. [16]. Here we present a brief summary of the method and the necessary equations required in the calculation of F_3 and F_4 in the high temperature limit:

$$F_3 = -\frac{(K_BT)^2}{12N}\sum_{\mathbf{q}_1 j_1}\sum_{\mathbf{q}_2 j_2}\sum_{\mathbf{q}_3 j_3}\Delta(\mathbf{q}_1 + \mathbf{q}_2 + \mathbf{q}_3)\frac{|\Phi(\mathbf{q}_1 j_1, \mathbf{q}_2 j_2, \mathbf{q}_3 j_3|^2}{\omega^2(\mathbf{q}_1 j_1)\omega^2(\mathbf{q}_2 j_2)\omega^2(\mathbf{q}_3 j_3)} \tag{17}$$

$$F_4 = +\frac{(K_BT)^2}{8N}\sum_{\mathbf{q}_1 j_1}\sum_{\mathbf{q}_2 j_2}\frac{\Phi(\mathbf{q}_1 j_1, \mathbf{q}_2 j_2, -\mathbf{q}_1 j_1, -\mathbf{q}_2 j_2}{\omega^2(\mathbf{q}_1 j_1)\omega^2(\mathbf{q}_2 j_2)} \tag{18}$$

$$\Phi(\mathbf{q}_1 j_1, \mathbf{q}_2 j_2, \mathbf{q}_3 j_3) = \frac{2}{M^{3/2}}\sum_{\mathbf{l}}{}'\sum_{\alpha\beta\gamma}\Phi_{\alpha\beta\gamma}(|\mathbf{r}^l|)e_\alpha(\mathbf{q}_1 j_1)e_\beta(\mathbf{q}_2 j_2)e_\gamma(\mathbf{q}_3 j_3)$$
$$\times [\sin(\mathbf{q}_1 \cdot \mathbf{r}^l) + \sin(\mathbf{q}_2 \cdot \mathbf{r}^l) + \sin(\mathbf{q}_3 \cdot \mathbf{r}^l)] \tag{19}$$

$$\Phi(\mathbf{q}_1 j_1, \mathbf{q}_2 j_2, -\mathbf{q}_1 j_1, -\mathbf{q}_2 j_2) = \frac{2}{M^2}\sum_{\mathbf{l}}{}'\sum_{\alpha\beta\gamma\delta} e_\alpha(\mathbf{q}_1 j_1)e_\beta(\mathbf{q}_2 j_2)$$
$$\times e_\gamma(-\mathbf{q}_1 j_1)e_\delta(-\mathbf{q}_2 j_2)\phi_{\alpha\beta\gamma\delta}(|\mathbf{r}^l|)[1 - \cos(\mathbf{q}_1 \cdot \mathbf{r}^l)][1 - \cos(\mathbf{q}_2 \cdot \mathbf{r}^l)] \tag{20}$$

In Eqs. (17)–(20), M is the atomic mass, $\omega(\mathbf{q}\,j)$ and $\mathbf{e}(\mathbf{q}\,j)$ are the eigenvalues and eigenvectors, respectively, for the wave vector $\mathbf{q}$ and branch index j; $\mathbf{r}^l = (a/2)[l_x, l_y, l_z]$, where a is the lattice constant and l_x, l_y, l_z are integer components of vector $\mathbf{l}$, whose sum is even for an fcc lattice; $\phi_{\alpha\beta\gamma}(|\mathbf{r}^l|)$ and $\phi_{\alpha\beta\gamma\delta}(|\mathbf{r}^l|)$ are the third and fourth rank tensor derivatives of $\phi(|\mathbf{r}|)$, respectively; the prime over the $\mathbf{l}$ summation indicates the omission of the origin point, and the indices α, β, γ, δ are each assigned the cartesian values x, y, z. The Δ function in Eq. (17) is unity if $\mathbf{q}_1 + \mathbf{q}_2 + \mathbf{q}_3$ is zero or a vector of the reciprocal lattice, and zero otherwise.

In the calculation of F_3 from Eqs. (17) and (19), we note that, although 27 terms are generated from the α, β, γ summations in Eq. (19), the symmetry of the $\phi_{\alpha\beta\gamma}(|\mathbf{r}^l|)$ tensor reduces them to 10. The complete expression for Eq. (19) has been presented in Eq. (12) of ref. [16], and we will not reproduce it here. However, we note that for a given $\mathbf{q}$ when the $\mathbf{l}$ summation is carried out in Eq. (19), the algebraic expressions for only three distinct terms need to be evaluated in the following function:

$$F_{\alpha\beta\gamma}(\mathbf{q}) = \sum_{\mathbf{l}}{}'\phi_{\alpha\beta\gamma}(|\mathbf{r}^l|)\sin(\mathbf{q} \cdot \mathbf{r}^l) \tag{21}$$

viz. $F_{xxx}(\mathbf{q})$, $F_{xxy}(\mathbf{q})$, and $F_{xyz}(\mathbf{q})$. The other 7 terms in the set of 10 terms can be obtained from these by a suitable change of indices. When the interaction extends to many neighbors, such as with long range potentials, the computational time can be reduced further by transforming the vector $\mathbf{l}$ sum in Eq. (21) to a shell summation involving the positive cartesian l_x^s, l_y^s, l_z^s components of the sth shell. An example of the $F_{xyz}(\mathbf{q})$ expression can be obtained from Eq. (14) of ref. [16]. The other terms can be obtained in a similar manner.

Once the function $F_{\alpha\beta\gamma}(\mathbf{q})$ is calculated, we calculate F_3 from Eq. (17) by the scanning method [31]. In the calculation of F_4, first we substitute Eq. (20) into (18) and isolate the following whole Brillouin zone (B.Z.)($\mathbf{q}$) and branch index (j) sums for a given $\mathbf{l}$, viz.

$$S_{\alpha\beta}(\mathbf{l}) = \sum_{\mathbf{q}j} \frac{e_\alpha(\mathbf{q}j)e_\beta(\mathbf{q}j)}{\omega^2(\mathbf{q}j)} \left[1 - \cos(\mathbf{q} \cdot \mathbf{r}^l)\right] \tag{22}$$

Next we write F_4 in terms of $S_{\alpha\beta}(\mathbf{l})$, i.e.,

$$F_4 = \frac{(k_BT)^2}{4NM^2} \sum_l{}' \sum_{\alpha\beta\gamma\delta} \Phi_{\alpha\beta\gamma\delta}(|\mathbf{r}^l|)\, S_{\alpha\beta}(\mathbf{l})\, S_{\gamma\delta}(\mathbf{l}) \tag{23}$$

The whole B.Z. sum in Eq. (22) is reduced to the irreducible 1/48th portion of the zone, and the j sum is carried out in terms of the Born's theorem by the method presented in Shukla and Wilk [32]. The symmetry of the tensors in the summand in Eq. (23) is such that the $\mathbf{l}$ sum can be simply changed to the shell(s) sum and the result multiplied with the multiplicity factor (n^s) of that shell. We do not reproduce the full form of the tensors $\Phi_{\alpha\beta\gamma}(|\mathbf{r}^l|)$ and $\Phi_{\alpha\beta\gamma\delta}(|\mathbf{r}^l|)$, as they are given in ref. [7].

5. RESULTS AND DISCUSSION

The results of the conversion of the adiabatic modulus B_s and its pressure derivative W_s to the corresponding isothermal quantities B and W obtained from each set of experimental specific heat data are shown in Table II. The differences between the two sets of isothermal quantities are small at 300 K, but rise to about 1% at 750 K. For the purpose of calculating $E(T)$ from Eq. (5), B is adequately represented by a linear dependence on T, while W is fitted by a second degree polynomial from which the derivatives W' and W'' are determined. For the data values used, the first three terms of Eq. (5) have comparable magnitudes and are much larger than the last four. The temperature dependence of these three terms is almost entirely due to the coefficients outside the brackets and, therefore, is determined by the variation of β, β', B, and B' with temperature.

Both β and β' increase as the temperature increases, while B decreases with essentially constant derivative B'. Thus it is possible that the sum of the three terms may change sign as the temperature is varied. Such an effect, mediated by the small contribution of the last four terms of Eq. (5), is shown in Table II, where $E(T)$ changes sign between 600 and 650 K.

The specific heat at the 0 K volume V_0 obtained from C_p by the application of Eqs. (1) and (5), contains a contribution from the conduction

Table II. Values of the Isothermal Bulk Modulus B (Pa) and Its Derivative $W = (\partial B/\partial p)_T$ Obtained from Table I, and the Specific Heat Data for C_p Given by Brooks and Bingham [2][a]

Part A

T (K)	$B \times 10^{-10}$	W	C_p (expt)	C_v (expt)	$E(T) \times 10^2$	C_{v_0}	ΔC_v
300	7.263	4.736	5.790	5.554	0.83	5.477	−0.483
350	7.122	4.767	5.983	5.688	1.19	5.596	−0.364
400	6.967	4.798	6.161	5.801	1.53	5.694	−0.266
450	6.801	4.830	6.311	5.880	1.80	5.759	−0.201
500	6.633	4.862	6.449	5.940	1.91	5.806	−0.154
550	6.454	4.894	6.591	5.997	1.69	5.854	−0.106
600	6.280	4.925	6.748	6.062	1.09	5.913	−0.047
650	6.098	4.957	6.918	6.131	−0.25	5.984	0.024
700	5.918	4.990	7.107	6.213	−2.41	6.076	0.116
750	5.740	5.023	7.309	6.301	−5.72	6.186	0.226
800	5.562	5.058	7.536	6.404	−10.5	6.325	0.365
850	5.381	5.093	7.812	6.549	−17.4	6.528	0.568

Part B[b]

T (K)	$B \times 10^{-10}$	W	C_p (expt)	C_v (expt)	$E(T) \times 10^2$	C_{v_0}	ΔC_v
300	7.260	4.742	5.741	5.505	0.80	5.428	−0.532
350	7.120	4.774	5.939	5.645	1.14	5.553	−0.407
400	6.963	4.807	6.095	5.736	1.47	5.629	−0.331
450	6.794	4.841	6.214	5.784	1.70	5.664	−0.296
500	6.627	4.873	6.367	5.859	1.78	5.727	−0.233
550	6.444	4.908	6.485	5.892	1.50	5.750	−0.210
600	6.268	4.942	6.624	5.939	0.84	5.793	−0.167
650	6.081	4.979	6.753	5.968	−0.60	5.825	−0.135
700	5.893	5.019	6.879	5.989	−2.90	5.858	−0.102
750	5.704	5.064	6.984	5.982	−6.44	5.874	−0.086

[a] C_v is the specific heat at volume $V(T)$, $E(T)$ is the correction $C_v(V(T), T) - C_v(V(0), T)$, C_{v_0} is $C_v(V(0), T)$ less the electronic contribution, and ΔC_v is $C_{v_0} - 3R$. All specific heats and $E(T)$ are in units of cal · mol^{-1} · K^{-1}.

[b] For Part B, data for C_p are from Leadbetter [1].

electrons. The tabulated specific heat C_{v_0} has been corrected by the usual free electron contribution, $C_e = 2.3 \times 10^{-4} T$, in cal · mol^{-1} · K^{-1}, corresponding to fixed volume V_0. The difference between C_{v_0} and $3R$, the high temperature limit of the harmonic contribution to the lattice specific heat, is tabulated as ΔC_v.

The error in C_{v_0} has three components. The first arises from the experimental error in C_p quoted in Section 2. The second component arises from the conversion of C_p to C_v via Eq. (1) and is estimated to be 3% of the difference, $C_p - C_v$. The third component arises from $E(T)$, and is estimated to be <15% of the mean absolute value of $E(T)$ on the basis of an examination of error propagation in Eq. (5) and by the fit of $E(T)$ to a third-order polynomial in T.

At temperatures above 700 K, vacancy formation is sufficient to affect the macroscopic properties of aluminum [20]. Accordingly, a contribution to the specific heat C_v^{vac} can be identified and is estimated by

$$C_v^{\text{vac}} = (Nk_B) \exp (\Delta S/k_B)(E/k_BT)^2 \exp -(E/k_BT) \qquad (24)$$

where E and ΔS are the energy and entropy of formation of a single vacancy, respectively. Estimates of C_v^{vac} for Al, using $E = 0.66$ eV and $(\Delta S/k_B) = 2.0$ [33], show that it is only 2% of C_{v_0} at 850 K.

In Fig. 1, we present C_{v_0} versus T, without correction for vacancies, for each data set. The error bars indicate the expected error from all sources. It is clear that the results of Brooks and Bingham, which rise above $3R$ between 600 and 650 K, are consistent with a positive anharmonic contribution to the specific heat. Correction for the effects of vacancies shifts the point at which $C_{v_0} > 3R$ to $T \simeq 650$ K. In contrast, the results of Leadbetter remain below $3R$ up to 750 K, and even on extrapolation do not rise above $3R$ until 850 K.

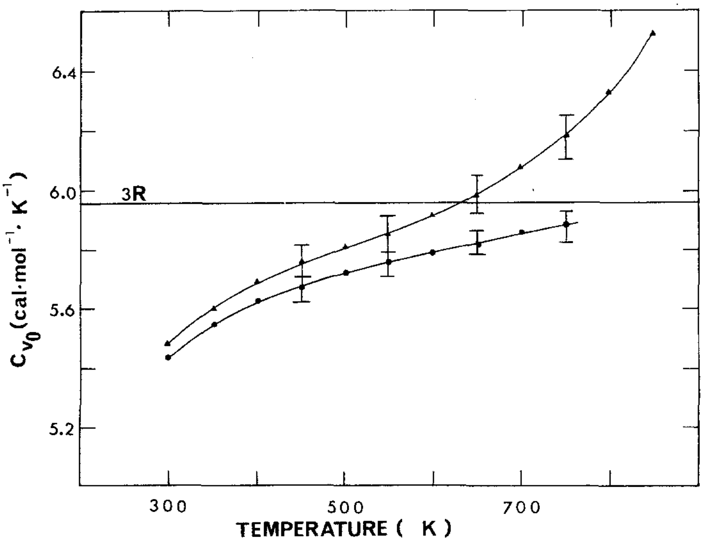

Fig. 1. The specific heat at constant volume reduced to 0 K volume (C_{v_0}) versus temperature (T): circles (●) for Leadbetter's data, and triangles (▲) for the Brooks and Bingham data.

Correction for the effects of vacancies keeps the extrapolated C_{v_0} below $3R$ up to the melting point.

In cases where C_{v_0} rises above $3R$, the magnitude of the anharmonic contribution can be determined from the following equation:

$$\Delta C_{v_0}/3R = (C_{v_0} - C_v^{\mathrm{vac}} - 3R)/3R, \tag{25}$$

where C_v^{vac} is given by Eq. (24), and the small difference between the high temperature harmonic contribution and $3R$ is neglected. We estimate ΔC_{v_0} from Eq. (25) for our analysis of the data of Brooks and Bingham, with $E = 0.66$ eV and $(\Delta S/k_B) = 2.0$ in Eq. (24). The variation of $\Delta C_v/3R$ with temperature is shown in Fig. 2, as well as the variation of the corresponding quantity determined by Brooks and Bingham [2]. Although the estimated anharmonic contribution does not follow a strictly linear variation with temperature, the curvature is slight. The mean slope is about 4×10^{-4} per K.

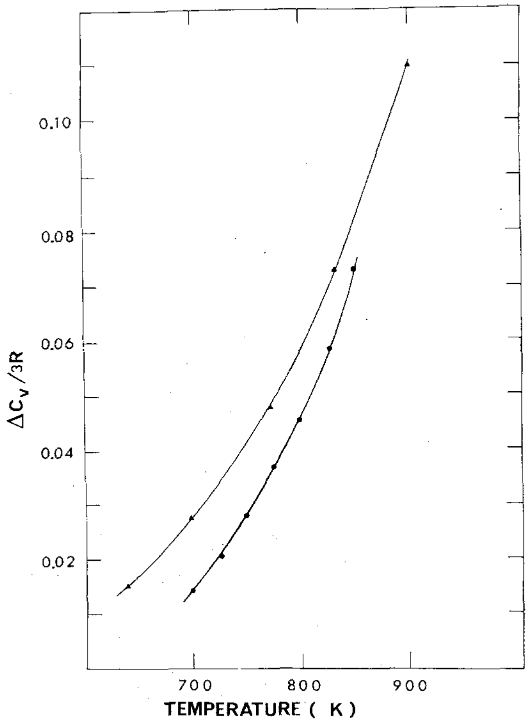

Fig. 2. The variation of $\Delta C_v/3R$ with temperature for the Brooks and Bingham data: circles (●) for our analysis, and triangles (▲) from ref. [2].

The same general behavior and slope is seen in both curves. Since Brooks and Bingham did not convert their C_v to C_{v_0}, some of the differences between these two curves can be attributed to this fact.

Now we summarize the results of the theoretical calculation of C_{v_0} (harmonic + anharmonic) from the three potentials presented in Section 3. The harmonic C_{v_0} is calculated from the well-known formula

$$C_{V_0}^h = k_B \sum_{\mathbf{q}j} \left| \frac{h\omega(\mathbf{q}\,j)}{2k_BT} \right|^2 \operatorname{cosech}^2 \left| \frac{h\omega(\mathbf{q}\,j)}{2k_BT} \right| \tag{26}$$

The high temperature expansion (three terms) gives the same results as Eq. (26) in the temperature range 550–900 K. The anharmonic contribution to C_{v_0}, $C_{v_0}^A$, is calculated in the high temperature limit from the F_3 and F_4 terms presented in Section 4. It is given by

$$C_{v_0}^A = -T\frac{\partial^2}{\partial T^2}(F_3 + F_4) = 3R(BT) \tag{27}$$

The essential ingredients in the calculation of $C_{v_0}^h$ and $C_{v_0}^A$ from the three potentials are the first four radial derivatives of $\Phi(r)$ evaluated at the various neighbor positions. In each case, these are evaluated numerically from the integral given by Eq. (9) and the corresponding $G(q)$ functions presented in Section 3.

The experimental values of $\omega(\mathbf{q}\,j)$ along the three principal symmetry and many off-symmetry directions are available from the neutron scattering work of Stedman and Nilsson [15]. Our calculated values of $\omega(\mathbf{q}\,j)$ from the

Table III. The Anharmonic Coefficient B in $C_{v_0}^A$ in Eq. (27) in Units of 10^{-6} K^{-1} for Different Potentials

	Number of shells		
Type of potential	In harmonic interaction	In anharmonic interaction	B
Dagens et al.[a]	28	28	21.87
Koehler et al.[b]	13	8	10.55
Ashcroft[c]	6	6	11.71
Morse	1	1	9.43
Rydberg	1	1	10.59

[a] M2 model pseudopotential with GT screening.

[b] Harrison modified point ion pseudopotential with Hubbard screening.

[c] Ashcroft pseudopotential with Hubbard screening.

first two derivatives of $\Phi(r)$ for the three cases agree to within a few percent with the observed values.

In Table III, we present the number of neighbors included in the harmonic and anharmonic interactions and the anharmonic coefficient B in Eq. (27) for the three potentials, along with the values of B for the Morse and Rydberg potentials from the recent work of R.C.S. [34]. For each potential, the coefficient is positive and an order of magnitude less than that determined by analysis of the experimental data of Brooks and Bingham. In all our calculations, $C_{v_0}^h$ was calculated, for each T, in the range 400–900 K from Eq. (26) employing 108,000 points in the whole Brillouin zone. F_3 and F_4 were calculated with 500 and 32,000 points in the whole zone, respectively.

We present in Fig. 3 the results of total C_{v_0} for the three potentials, where the anharmonic contribution was added to $C_{v_0}^h$ for $T \geq 500$ K and forms less than 1% of C_{v_0}. In this figure, we also present the two sets of experimental C_{v_0} values in which allowance has been made for vacancy formation for $T \geq 700$ K.

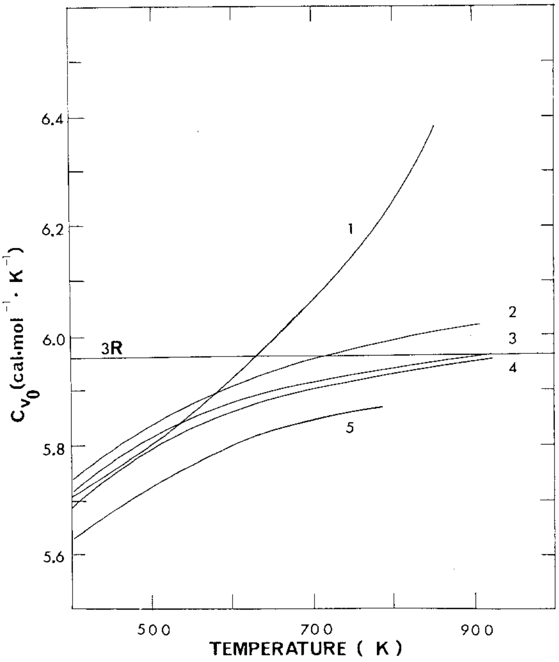

Fig. 3. Calculated C_{v_0} versus T for the three potentials and the two experimental curves. Curve 1, Brooks and Bingham; curve 2, Dagens et al. potential; curve 3, Ashcroft potential; curve 4, Harrison modified point ion potential; curve 5, Leadbetter's data.

It is clear from this figure that for all three potentials, the approach of C_{v_0} to the value $3R$ is very slow. The C_{v_0} obtained from the Dagens et al. potential reaches $3R$ at 700 K, whereas the other two theoretical C_{v_0}'s barely approach $3R$ about 900 K. The C_{v_0} curve for the Koehler et al. and Ashcroft potentials almost overlap each other in the temperature range 400–900 K. It is to be noted that both potentials are obtained from the Hubbard exchange and correlation function in $\epsilon(q)$, whereas the Dagens et al. potential employs the GT screening function. Thus the main difference between the curves appears to arise from the use of different exchange and correlation factors.

The difference between the C_{v_0} curve from the analysis made of the Brooks and Bingham data and the theoretical curves is marked. It appears that the experimental points are too high from about 500 K up. The C_{v_0} curve from the analysis of Leadbetter's data is very similar to the form predicted for each of the three potentials, but the results appear to be too low. The Monte Carlo points of C_{v_0} calculated by Mountain and Knauss [14] lie above $3R$ for 500 and 600 K and below for 700 K.

6. CONCLUSIONS

We conclude that the anharmonic contribution to the specific heat of aluminum predicted by theory for the potentials considered here is positive. The apparent agreement of sign of the specific heat contribution of Brooks and Bingham with this conclusion should not be taken as confirmation of the predictions because of possible errors in their results. The disagreement between the results of Leadbetter and Brooks and Bingham increases as the temperature increases, although the two sets of data were in reasonable agreement from 300 to 500 K. There appears to be a need for remeasurement of the specific heat of aluminum from 500 K to the melting point.

ACKNOWLEDGMENTS

The authors would like to thank Mrs. Joyce Cowan for careful typing of this manuscript, and R. C. Shukla acknowledges the financial support of this work from the Natural Sciences and Engineering Research Council of Canada.

REFERENCES

1. A. J. Leadbetter, *J. Phys. C (Proc. Phys. Soc.)* **1:**1481 (1968).
2. C. R. Brooks and R. E. Bingham, *J. Phys. Chem. Solids* **29:**1553 (1968).
3. A. J. Leadbetter, *J. Phys. C (Proc. Phys. Soc.)* **1:**1489 (1968).
4. R. E. Peierls, *Quantum Theory of Solids* (Oxford University Press, New York, 1955).
5. E. A. Stern, *Phys. Rev.* **111:**786 (1958).

6. W. Ludwig, *J. Phys. Chem. Solids* **4**:283 (1958).
7. A. A. Maradudin, P. A. Flinn, and R. A. Coldwell-Horsfall, *Ann. Phys. (N.Y.)* **15**:337 (1961); **15**:360 (1961).
8. R. C. Shukla and E. R. Muller, *Phys. Status Solidi* **43**:413 (1971).
9. J. C. Slater, *Introduction to Chemical Physics* (McGraw-Hill, New York, 1939), Chapter XIII.
10. W. C. Overton, J. Chem. Phys. **37**:2975 (1962).
11. W. A. Harrison, *Pseudopotentials in the Theory of Metals* (Benjamin, New York, 1966).
12. L. Dagens, M. Rasolt, and R. Taylor, *Phys. Rev.* **B11**:2726 (1975).
13. T. R. Koehler, N. S. Gillis, and D. C. Wallace, *Phys. Rev.* **B1**:4521 (1970).
14. R. D. Mountain and D. C. Knauss, *J. Res. Natl. Bur. Stand.* **85**:109 (1980).
15. R. Stedman and G. Nilsson, *Phys. Rev.* **145**:492 (1966).
16. R. C. Shukla and R. Taylor, *Phys. Rev.* **89**:4116 (1974).
17. W. C. Overton, *J. Chem. Phys.* **37**:116 (1962).
18. D. B. Fraser and A. C. Hollis-Hallett, *Can. J. Phys.* **43**:193 (1965).
19. D. F. Gibbons, *Phys. Rev.* **112**:136 (1958).
20. R. O. Simmons and R. W. Balluffi, *Phys. Rev.* **117**:52 (1960).
21. D. Gerlich and E. S. Fisher, *J. Phys. Chem. Solids* **30**:1197 (1969).
22. J. F. Thomas, *Phys. Rev.* **175**:955 (1968).
23. R. E. Schmunk and C. S. Smith, *J. Phys. Chem. Solids* **9**:100 (1959).
24. M. S. Duesbery and R. Taylor, *Phys. Rev.* **B7**:2870 (1973).
25. P. V. S. Rao, *J. Phys. Chem. Solids* **35**:669 (1974).
26. K. S. Singwi, A. Sjolander, M. P. Tosi, and R. H. Land, *Phys. Rev.* **B1**:1044 (1970).
27. D. J. W. Geldart and R. Taylor, *Can. J. Phys.* **48**:167 (1970).
28. P. Vashishta and K. S. Singwi, *Phys. Rev.* **B6**:875 (1972).
29. D. C. Wallace, *Phys. Rev.* **187**:991 (1969).
30. L. Dagens, M. Rasolt, and R. Taylor, T.P. 579, A.E.R.E., Harwell (June 1974).
31. P. A. Flinn and A. A. Maradudin, *Ann. Phys.* (N.Y.) **22**:223 (1963).
32. R. C. Shukla and L. Wilk, *Phys. Rev.* **B10**:3660 (1974).
33. W. Triftshaüser, *Phys. Rev.* **B12**:4634 (1975).
34. R. C. Shukla, *Int. J. Thermophys.* **1**:73 (1980).